Research Article

Phytochemical Analysis

Received: 25 March 2010; Revised: 15 June 2010; Accepted: 20 June 2010 Published online in Wiley Online Library: 2 November 2010

(wileyonlinelibrary.com) DOI 10.1002/pca.1271

GC-MS Analysis of Headspace and Liquid Extracts for Metabolomic Differentiation of Citrus Huanglongbing and Zinc Deficiency in Leaves of 'Valencia' Sweet Orange from Commercial Groves

Juan Manuel Cevallos-Cevallos, Rosalía García-Torres, Edgardo Etxeberria and José Ignacio Reyes-De-Corcuera*

ABSTRACT:

Introduction – Citrus Huanglongbing (HLB) is considered the most destructive citrus disease worldwide. Symptoms-based detection of HLB is difficult due to similarities with zinc deficiency.

Objective – To find metabolic differences between leaves from HLB-infected, zinc-deficient, and healthy 'Valencia' orange trees by using GC-MS based metabolomics.

Methodology – Analysis based on GC-MS methods for untargeted metabolite analysis of citrus leaves was developed and optimized. Sample extracts from healthy, zinc deficient, or HLB-infected sweet orange leaves were submitted to headspace solid phase micro-extraction (SPME) and derivatization treatments prior to GC-MS analysis.

Results – Principal components analysis achieved correct classification of all the derivatized liquid extracts. Analysis of variance revealed 6 possible biomarkers for HLB, of which 5 were identified as proline, β-elemene, (-)trans- caryophyllene, and α-humulene. Significant ($P < 0.05$) differences in oxo-butanedioic acid, arabitol, and neo-inositol were exclusively detected in samples from plants with zinc deficiency. Levels of isocaryophyllen, α-selinene, β-selinene, and fructose were significantly ($P < 0.05$) different in healthy leaves only.

Conclusion – Results suggest the potential of using identified HLB biomarkers for rapid differentiation of HLB from zinc deficiency. Copyright © 2010 John Wiley & Sons, Ltd.

Keywords: Huanglongbing; metabolomics; biomarker; GC-MS; citrus; zinc deficiency

Introduction

Citrus Huanglongbing (HLB) is considered the most destructive citrus disease worldwide (Callaway, 2008). The devastating effect of HLB on citrus production in Africa, Asia, and the Americas has been well documented (Chung and Brlansky, 2005), and the importance of this disease has triggered several reviews of HLB in countries such as Pakistan (Batool *et al.*, 2007), India (Das, 2008), Malaysia (Hajivand *et al.*, 2009), as well as Brazil and US (Gottwald *et al.*, 2007). HLB affects most citrus varieties including 'Valencia' sweet orange. 'Valencia' orange is the most widely cultivated citrus variety in the world (Papadakis *et al.*, 2008). Therefore, HLB effects in this variety have the potential of causing serious economical loses.

Citrus HLB is thought to be caused by '*Candidatus* Liberibacter spp' bacteria transmitted by the psyllids *Diaphorina citri* and *Trioza erytreae* (Bove, 2006). Symptoms of HLB are characterized by chlorosis in leaves (marked by large yellow areas) as well as small, misshapen, and inedible fruits (Halbert and Manjunath, 2004). Symptoms-based identification of HLB is difficult mainly due to foliar similarities with zinc deficiency (ZD) (supplementary Figure 1) (Albrecht and Bowman, 2008). Additionally, ZD is one of the most common conditions that produces chlorosis in citrus (Zekri and Obreza, 2003) similar to HLB. Other pathological and physiological conditions that produce chlorosis in citrus are uncommon or show significantly different symptoms from those of HLB and ZD. Because of its sensitivity, PCR is currently the only method that specifically detects HLB, and thus differentiates this disease from ZD. However, low concentration and uneven distribution of the bacteria in infected tree (McClean, 1970) as well as the weak DNA amplification of '*Candidatus* Liberibacter spp' during spring and summer (Gopal *et al.*, 2007b) make PCR diagnosis difficult. Additionally, PCR techniques are costly, laborious, time consuming and cannot be used for in-field testing. In spite of recent improvements to PCR methods (Ding *et al.*, 2007; Gopal *et al.*, 2007a; Kawai *et al.*, 2007; Urasaki *et al.*, 2008) and the

* Correspondence to: José I. Reyes-De-Corcuera, 700 Experiment Station Rd., Lake Alfred, FL 33850. E-mail: jireyes@ufl.edu, Phone: 863-956-1151 x 1344, Fax: 863-956-4631

University of Florida, IFAS, Citrus Research and Education Center, Lake Alfred, FL

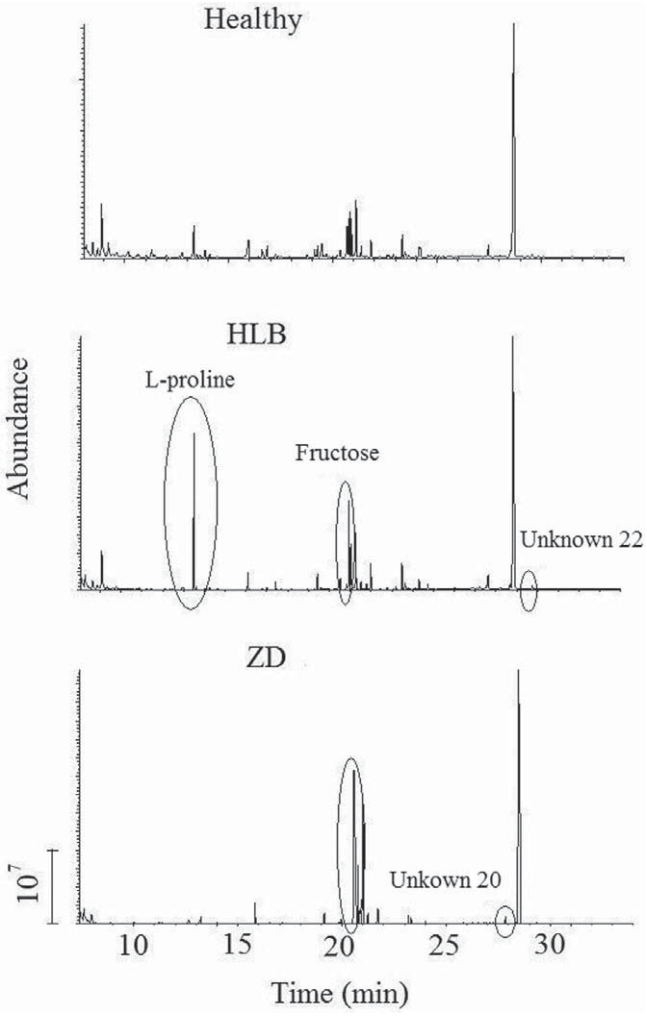

Figure 1. Typical chromatograms of derivatized liquid extracts of healthy, HLB-infected, and zinc deficient leaves. Circled compounds represent visible significant differences.

development of culture media for the growth of pure (Sechler *et al.*, 2009) and co-cultivated (Davis *et al.*, 2008) '*Candidatus* Liberibacter spp'; rapid, inexpensive, reliable, and portable methods for HLB detection are still unavailable.

Metabolite-based methods (chemical assays that target a specific metabolite) may become an inexpensive alternative for HLB in-field diagnosis. Metabolites such as starch (Takushi *et al.*, 2007a) and gentisic acid (Hooker *et al.*, 1993) have been reported to accumulate abnormally in HLB-infected trees and were presented as an alternative for diagnosis because of their easy-to-perform quantification methods. However, increased amounts of starch (Li *et al.*, 2003) and gentisic acid (Belles *et al.*, 2006) have also been found with non-HLB conditions such as girdling and other plant diseases. The non-specificity of these compounds has triggered the search of new biomarkers for HLB. Metabolomic discovery of new HLB-biomarkers is likely to trigger the development of rapid, portable, and inexpensive assays such as chemical detection kits, sensors, and biosensors for HLB screening.

Metabolite profiling of healthy and HLB-infected leaves of sweet orange by metabolomic techniques based on HPLC-MS (Cevallos-Cevallos *et al.*, 2008; Manthey, 2008) and capillary electrophoresis-photo diode array detector (Cevallos-Cevallos *et al.*, 2009b) reported several flavonoid-type compounds and hydroxycinnamates as possible biomarkers. However, samples with ZD were not analyzed and specificity of suggested biomarkers was not reported. Metabolomics techniques represent an option to finding new HLB biomarkers and determining their specificity by comparing metabolite profile of HLB-infected, ZD-affected, and healthy plants. Besides HPLC and capillary electrophoresis, metabolomic analyses by GC-MS provide an alternative for detecting less polar and low molecular weight compounds (Fancy and Rumpel, 2008) and have been shown to be a powerful tool for metabolite profiling in plants. This kind of studies are considered as targeted metabolomics because they are aimed at those compounds detectable by GC-MS (Cevallos-Cevallos *et al.*, 2009a; Sawada *et al.*, 2009). Additionally, metabolomic discrimination in plants can be achieved without the need of compound identification (Hall *et al.*, 2002) increasing differentiation power by including unknown compounds. Abu-Nada *et al.*, (2007) suggested specific metabolite variations during several stages of *Phytophthora infestans* infection in potato leaf extracts using GC-MS. Additionally, metabolite changes due to stress conditions such as drought (Semel *et al.*, 2007) and wounding (Yang and Bernards, 2007) have been quantified by GC-MS analyses of tomato and potato plants, respectively. In most of the GC-MS-based metabolomics reports, liquid extracts have been dried and derivatized prior to analysis in order to increase detection of more polar compounds (Fancy and Rumpel, 2008). However, drying may cause substantial losses of the highly volatile compounds usually found in the sample's headspace. These highly volatile compounds have been shown to play an important role in metabolite profiling of several plant stresses and diseases (Tikunov *et al.*, 2007). As an example, GC-MS profiling of headspace metabolites allowed differentiation of two fungal diseases in mangoes (Moalemiyan *et al.*, 2007). Similarly, headspace analysis of tomato plants permitted determination of changes in metabolites occurring after infection with tomato mosaic virus (Deng *et al.*, 2004). In spite of the individual importance of these two types of analysis, no combined headspace and liquid extracts analyses of plant diseases have been reported. Additionally, no GC-MS-based metabolomic analyses of HLB-infected plants, as well as no comparison between HLB and zinc deficient metabolite profiles in sweet orange leaves have been reported.

The objective of this study was to find metabolic differences between leaves from HLB-infected, zinc-deficient, and healthy 'Valencia' orange trees from commercial groves as a first step to identify potential HLB biomarkers by combined GC-MS analysis of headspace and derivatized liquid extracts.

Experimental

Reagents

All HPLC grade reagents (methanol and chloroform), L-proline, L-threonine, L-alanine, arabitol, inositol, butanedioic acid, methoxyamine hydrochloride (20 mg mL^{-1}) in pyridine (MOX), and *N*-methyl-*N*-trimethylsilyl trifluoroacetamide (MSTFA) were purchased from Fisher Scientific Inc. (Pittsburg, PA, USA). Trans-Caryophyllene, isocaryophyllene, and α-humulene were from Sigma-Aldrich (Saint Louis, MO, USA).

Equipment and software

The GC model HP 5890 coupled to an HP 5971 series quadrupole mass spectrometer with ChemStation B.02.02 data acquisition software and the Wiley 138 K mass spectral database were from Hewlett Packard (Palo Alto, CA, USA). Sensitivity and reproducibility of liquid extracts and

headspace volatile analyses were maintained by regular cleaning of the ion source (approx once a month) and verified by daily running known concentrations of pure standards in the GC-MS. The chromatographic column used for both headspace and liquid extract analyses was a DB5-MS 60 m × 0.25 mm × 0.25 μm (length × I.D.x film thickness) from J & W Scientific (Folsom, CA, USA). The water bath (model Isotemp 3016 s) and sonicator (model FS20H) were from Fisher Scientific (Pittsburg, PA, USA). Data was aligned to correct deviations in retention time by using MetAlign software (www.metalign.nl) and normalized to the total area prior to principal components analysis (PCA). Compounds were tentatively identified as described in the compound identification section prior to analysis of variance (ANOVA). PCA was run to compare the overall metabolite profile of the samples and ANOVA was run to determine significance of individual compounds. Additionally, ANOVA of peak areas was performed for each detected compound in all samples and for all analyses. Principal components analysis and ANOVA were carried out using MATLAB R2008a from The MathWorks (Natick, MA, USA) and significant differences were reported at 95% confidence level. Both PCA and ANOVA were run on the peak intensities, similar to what was done in previous studies (Abu-Nada *et al.*, 2007; Moalemiyan *et al.*, 2007; Semel *et al.*, 2007)

Sampling and experimental design

'Valencia' sweet orange was chosen for this study because it is the most widely cultivated citrus variety in the world. Leaves of healthy and symptomatic HLB-infected (PCR positive) 'Valencia' sweet orange trees were sampled in commercial groves located in Plant City (grove 1) and Lake Alfred (grove 2), FL and leaves from trees showing ZD were collected from research trees at a University of Florida's Citrus Research and Education Center (CREC) grove in Lake Alfred, FL, USA. Huanglongbing-infected samples were taken approximately 3 months and 3 weeks after symptoms were first noticed for groves 1 and 2 respectively. All sampled leaves were from trees of the same age and similar shoots (spring and summer shoots from 10-year-old trees). Samples were kept on dry ice during collection and transport (45 min approximately), and then stored at −80°C until analyzed (approximately 2 months). To confirm HLB infection, PCR analyses were outsourced to the Plant Pathology Laboratory at the CREC in Lake Alfred, FL, USA. At least six leaves from three different PCR-positive, PCR-negative (healthy), and ZD-affected trees were sampled monthly from November 2007 to October 2008 to assess seasonal variability. After using some of the samples for PCR analyses and GC-MS optimization experiments, 36 HLB-infected, 28 ZD-affected, and 18 healthy leaves were individually analyzed.

Extraction conditions

Extraction conditions were similar to those previously reported for HLB metabolite profiling in capillary electrophoresis (Cevallos-Cevallos *et al.*, 2009b) with some modifications. Briefly, individual leaves (≈0.45 g) were ground to a fine powder with liquid nitrogen. Approximately 15 mg of L-threonine were added as a first internal standard (IS1). Solvent was added to a final concentration of 4% w/v of ground tissue. Solvent was a methanol/water/chloroform combination suggested by Gullberg et al. (2004) in a 8:1:1 ratio and was added within one minute of grinding to stop degradation reactions. The mixture was sonicated on ice for 10 min. The extraction were done overnight at 0°C in the temperature-controlled water bath. After extraction samples were filtered using 0.45 μm nylon syringe filters and (E,E,)-2,4 nonadienal was added to a final concentration of 800 mg L^{-1} as second internal standard (IS2). IS1 and IS2 were added as quality control of the derivatization and headspace extraction respectively as well as to assure adequate GC-MS analysis and library matching. Endogenous IS1 and IS2 were not detected in either sample category under tested conditions, and did not interfere with any peaks in the chromatograms. Extraction with pure chloroform and pure methanol overnight at 0°C were also tested but yielded significantly less peaks than the combination methanol/water/chloroform described above and therefore were not used for this study (see results and discussion section).

Headspace analysis

A solid phase micro-extraction (SPME) fiber 50/30 μm DVB/Carboxen ™/PDMS StableFlex ™ for manual holder 57328-U from Supelco (Bellefonte, PA, USA) was conditioned prior to its first use at 270°C for 1 h, and at the start of every day at 240°C for 5 min. Fifteen milliliters of the samples extracted with methanol/water/chloroform 8:1:1 were transferred to a 50 mL vial and equilibrated at 40°C for 30 min while stirred. The preconditioned SPME fiber was exposed to the headspace of the equilibrated samples for 40 min at 40°C and then splitlessly injected into the GC-MS. The injector temperature was 240°C, the oven was initially held at 55°C for 1 min, the temperature rate was 7°C min^{-1}, and the final temperature was 260°C held for 5 min. Ultrapure hydrogen was used as the carrier gas at 1 mL min^{-1}. The MS was tuned to maximum sensitivity in electron impact mode, positive polarity, and the total ion current was recorded for a mass range of 25–650 amu. The GC-MS interface was set to 318°C. The scan was recorded after a solvent delay of 8 min with scan frequency of 4 s^{-1}.

Liquid extract analyses

For liquid extracts, 180 μL were transferred into a 1-mL GC vial and dried under a nitrogen flow. To the dried extract 30 μL MOX were added and allowed to react for 17 h at room temperature. Other combinations of time and temperature showed lower reproducibility as reported in similar studies (Gullberg *et al.*, 2004). After methoximation with MOX, silylation reactions were induced by adding 80 μL of MSTFA for 2 h at room temperature. Other times and amounts of MSTFA yielded lower number of detected peaks and poorer reproducibility (see results and discussion section). Volumes of 0.3 μL of derivatized sample were splitlessly injected into the GC-MS. The injector was at 250°C, the initial oven temperature was 70°C held for 1 min, the temperature rate was 10°C min^{-1}, and the final temperature was 315°C held for 10 min. After 8 min of solvent delay the total ion current of mass fragments in the range of 50–650 amu was recorded. Other MS conditions were identical to that used for headspace analysis.

Compound identification

Mass spectra obtained were visually observed at the beginning, middle, and end width of each peak to detect coelution. No coelution was detected in any of the peaks. Compound identification was done by library matching of mass spectra using the Wiley library and our internal databases. Compound identity was obtained and reported in Tables 2 and 3 only when the matching value of the mass spectra comparison was 70 or higher and an increase in the size of the peak was observed when spiking the sample with the corresponding pure standard. Additionally, the linear retention index (LRI) was reported for each compound detected. A series of alkanes from C8 (LRI = 800) to C20 (LRI = 2000) were run under the GC-MS conditions set for both liquid extracts and headspace volatiles. Linear retention indices were estimated by direct correlation with the retention times of the alkanes.

Preliminary validation of possible HLB biomarkers

Preliminary validation was done using training and validation groups of samples from each of the previously described groves, as performed in other metabolomic studies (Ikeda *et al.*, 2007; Pongsuwan *et al.*, 2008; Tarachiwin *et al.*, 2007). The validation group consisted of ten samples of each treatment (HLB, ZD, and healthy) taken from each of the two groves and analyzed as described in previous sections. ANOVA was run on each compound to determine significance of the potential biomarkers. Peak areas as well as infected-healthy and infected-zinc deficiency ratios were compared between groves. Additionally, non symptomatic leaves from HLB-infected trees were analyzed following the methodology previously described and suitability of suggested biomarkers for pre-symptomatic HLB differentiation was proposed. PCR analyses of both symptomatic and non-symptomatic leaves were also performed.

Results and Discussion

Extraction and derivatization conditions

Polar extracts obtained with pure methanol were compared to chloroform and methanol/water/chloroform (8:1:1) extracts. No significant differences were found when comparing chloroform extracts from healthy and HLB-infected leaves confirming previous observations that non-polar compounds are less likely candidates for fingerprinting in plant metabolomic analyses (Cevallos-Cevallos *et al.*, 2009a). Samples from healthy and HLB-infected trees showed significant differences when extracted with pure methanol and with the combination methanol/water/chloroform (8:1:1). However, the 8:1:1 mixture yielded a higher number and greater concentration of peaks (Supplementary Figure 2) and therefore was used as the extraction media for this study. Results were in accordance to previously reported data for HLB fingerprinting using capillary electrophoresis (Cevallos-Cevallos *et al.*, 2009b).

Amount of silylation reagent and duration of the reaction are the two known concerns that need to be addressed prior application of a derivatization methodology (Kanani *et al.*, 2008). Several derivatization conditions were tested by adding MSTFA from 40 µL to 120 µL (20 µL intervals) during 40, 80, 120, 160, and 200 min. The amount of the silylation agent MSTFA added caused a significant effect on the 11 compounds reported in Table 1 and Supplementary Figure 3. The derivatized form of glucose, galactose oxime, and mannitol (Supplementary Figure 3) as well as L-proline, unknown 6, and inositol (Table 1) showed a maximum peak area after reacting with 80 µL of MSTFA. Lower and higher amounts of MSTFA caused a reduction in peak areas probably due to incomplete derivatization and dilution effect respectively. Conversely, the derivatized form of glucitol (Supplementary Figure 3), unknown 5, glutamic acid, and glycine (Table 1) showed a maximum peak area when reacting with 40 µL of MSTFA. Higher levels of MSTFA caused a reduction in their peak areas, probably due to a dilution effect. All compounds were detectable at both 40 and 80 µL of MSTFA but the latter showed the lowest standard error and improved reproducibility (Table 1 and Supplementary Figure 3) and was chosen for this study.

Variation in MSTFA reaction time significantly affected six compounds only (Supplementary Figure 4). The lowest standard error and better reproducibility were observed between 80 and 150 min of reaction. Therefore, a reaction time of 120 minutes was selected for the metabolomics study. Adding 80 µL of MSTFA followed by a reaction time of 120 min yielded the best compromise between peak area and reproducibility.

GC-MS analyses of derivatized samples

Figure 1 shows typical chromatograms of samples from healthy, HLB-infected, and ZD-affected trees from groves 1 and 2. Data was aligned and normalized to the total area prior to statistical analysis. Principal component analysis was carried out to compare the overall metabolite profile of each sample group. Figure 2A shows that PCA was able to classify all the samples according to their initial physiological condition, suggesting marked differences in the metabolite profile of each sample

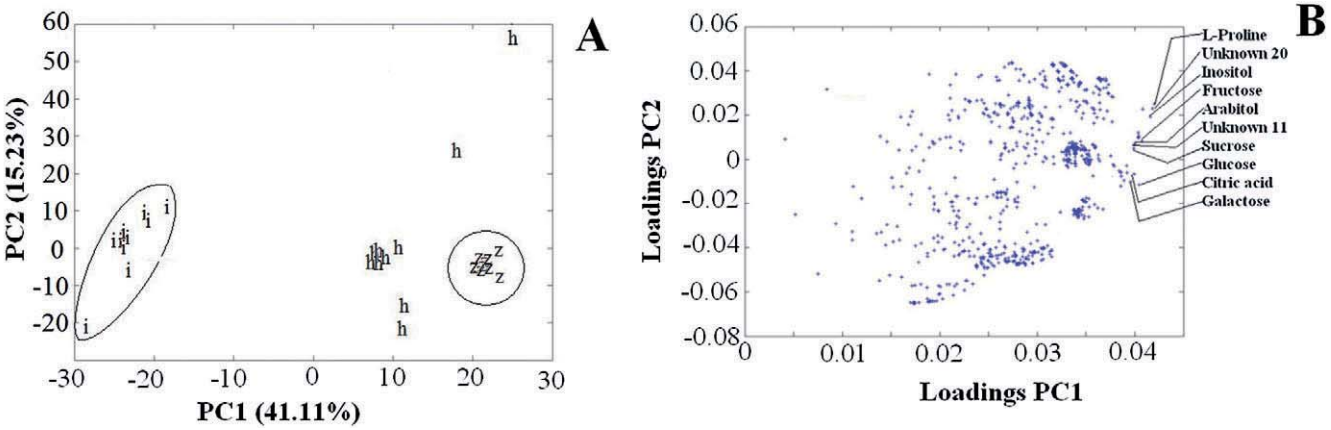

Figure 2. Principal components analysis of derivatized liquid extracts. (A) Score plot of HLB-infected (i), healthy (h), and zinc deficient (z) samples illustrated in PC1 and PC2. (B) Loading plot of PC1 and PC2. The 10 compounds with the highest loadings on PC1 are marked.

Table 1. Effect of amount of MSTFA added on the normalized peak area of compounds expressing the highest variation*

Compound	Normalized peak area for selected amounts of MSTFA				
	40 µL	60 µL	80 µL	100 µL	120 µL
Unknown 5	5590 +/– 193	3356 +/– 553	2878 +/– 237	1418 +/– 249	1786 +/– 245
Unknown 6	3371 +/– 356	3925 +/– 488	3849 +/– 260	2845 +/– 186	2419 +/– 190
L-proline 2TMS	5179 +/– 222	13662 +/– 738	12120 +/– 153	10189 +/– 340	8349 +/– 327
L-glutamic acid, TMS	12120 +/– 1157	10649 +/– 472	9604 +/– 344	7437 +/– 472	6449 +/– 300
L-glycine,TMS	7702 +/– 3952	7188 +/– 1610	6340 +/– 861	4478 +/– 228	3819 +/– 317
Inositol 6TMS	7907 +/– 8570	8785 +/– 2989	8897 +/– 2099	6402 +/– 1940	5653 +/– 1380

* Values are averages of normalized peak area +/– standard error.

Table 2. Main compounds detected in derivatized samples*

Linear Retention Index (LRI)	Tentative identity	Relative abundance (%) ZD	HLB	Healthy
967	UN1	0,177 +/– 0,005	0,192 +/– 0,004	0,121 +/– 0,003
979	Benzene, 1,2,5-trimethyl	1,400 +/– 0,026	1,198 +/– 0,022	0,593 +/– 0,016
994	Tetrasiloxane, decamethyl	0,048 +/– 0,001	0,076 +/– 0,001	0,218 +/– 0,005
1004	UN2	0,037 +/– 0,001	0,074 +/– 0,001	0,017 +/– 0,000
1020	Butanoic acid, 2-[(trimethylsilyl)oxy	0,153 +/– 0,004	0,201 +/– 0,004	0,130 +/– 0,003
1024	UN3	0,030 +/– 0,001	0,017 +/– 0,001	0,057 +/– 0,001
1030	UN4	0,006 +/– 0,000	0,002 +/– 0,000	0,000 +/– 0,000
1062	L-Alanine, N-(trimethylsilyl)-, trime	0,055 +/– 0,001	0,038 +/– 0,001	0,004 +/– 0,000
1134	UN5	0,034 +/– 0,001	0,316 +/– 0,007	0,057 +/– 0,001
1206	3,7-Dioxa-2,8-disilanonane, 2,2,8,8-t	0,025 +/– 0,001	0,038 +/– 0,001	0,100 +/– 0,001
1212	UN6	0,374 +/– 0,006	0,462 +/– 0,005	0,421 +/– 0,003
1248	L-Proline 2TMS	1,257 +/– 0,014	4,258 +/– 0,038[a]	0,928 +/– 0,008
1280	UN7	0,141 +/– 0,003	0,078 +/– 0,001	0,271 +/– 0,003
1294	L-Serine TMS	0,136 +/– 0,002	0,220 +/– 0,002	0,191 +/– 0,001
1406	Butanedioic acid, [(trimethylsilyl)ox	3,009 +/– 0,043	1,802 +/– 0,025	3,028 +/– 0,020
1451	L-glutamic acid, N-(trimethylsilyl)-	0,272 +/– 0,003	0,226 +/– 0,003	0,315 +/– 0,003
1462	Glycine, N,N-bis(trimethylsilyl)-	0,135 +/– 0,002	0,402 +/– 0,007	0,841 +/– 0,009
1468	Tetronic acid TMS	0,071 +/– 0,002	0,000 +/– 0,000	0,000 +/– 0,000
1486	UN8	0,123 +/– 0,001	0,391 +/– 0,006	0,176 +/– 0,001
1519	UN9	0,001 +/– 0,000	0,007 +/– 0,000	0,016 +/– 0,000
1599	Arabitol TMS	ND[a]	0,166 +/– 0,002	0,209 +/– 0,002
1609	UN10	0,395 +/– 0,004	1,020 +/– 0,011	0,473 +/– 0,006
1617	UN11	0,103 +/– 0,002[a]	0,397 +/– 0,005[a,b]	0,675 +/– 0,007[b]
1623	UN12	0,149 +/– 0,002[a]	0,065 +/– 0,001[a,b]	0,027 +/– 0,001[b]
1670	Citric acid 4TMS	0,096 +/– 0,002	0,015 +/– 0,000	0,008 +/– 0,000
1675	1-(4′-Trimethylsilyloxyphenyl)-1-Trime	0,194 +/– 0,003	0,472 +/– 0,007	0,228 +/– 0,002
1701	UN13	18,930 +/– 0,229	5,513 +/– 0,054	3,381 +/– 0,091
1707	Fructose 5TMS	5,141 +/– 0,058[a]	7,429 +/– 0,140[a]	0,608 +/– 0,007
1716	D-gluco-hexodialdose, 4TMS	0,130 +/– 0,001	0,203 +/– 0,005	0,029 +/– 0,001
1721	D-Mannitol 6TMS	20,334 +/– 0,151	11,780 +/– 0,184	5,365 +/– 0,050
1740	Galactose oxime 6TMS	0,600 +/– 0,010	0,397 +/– 0,010	0,006 +/– 0,000
1764	Inositol 6TMS	0,190 +/– 0,002[a]	1,299 +/– 0,013	1,844 +/– 0,015
1789	Galactonic acid 6TMS	0,027 +/– 0,000[a]	0,088 +/– 0,002[a,b]	0,175 +/– 0,002[b]
1811	UN14	0,118 +/– 0,004	0,173 +/– 0,002	0,282 +/– 0,002
1855	Myo-Inositol 6TMS	0,570 +/– 0,006	1,019 +/– 0,008	0,907 +/– 0,005
1864	D-Glucitol 6TMS	0,349 +/– 0,004	0,564 +/– 0,007	0,300 +/– 0,002
1894	UN15	0,012 +/– 0,000[a]	0,099 +/– 0,001	0,062 +/– 0,000
1905	Glucose 5TMS	0,260 +/– 0,003	0,734 +/– 0,011	0,544 +/– 0,009
2043	UN16	0,127 +/– 0,002	0,140 +/– 0,002	0,088 +/– 0,001
2047	UN17	0,127 +/– 0,002	0,045 +/– 0,001	0,117 +/– 0,001
2063	UN18	0,182 +/– 0,003[a]	0,128 +/– 0,002[a]	0,009 +/– 0,000
2081	Butanedioic acid, oxo (TMS)	0,176 +/– 0,003[a]	0,000 +/– 0,000	0,000 +/– 0,000
2091	UN19	0,125 +/– 0,002	0,067 +/– 0,001	0,170 +/– 0,002
2096	Butanedioic acid, oxo (TMS)	0,182 +/– 0,004	0,052 +/– 0,001	0,026 +/– 0,001
2147	UN20	0,181 +/– 0,003[a]	0,051 +/– 0,001	0,006 +/– 0,000
2175	Sucrose TMS	26,443 +/– 0,254	46,378 +/– 0,354	55,111 +/– 0,262
2188	UN 21	0,002 +/– 0,000	0,034 +/– 0,001	0,000 +/– 0,000
2240	UN22	0,023 +/– 0,001	0,186 +/– 0,003[a]	0,032 +/– 0,001

* Values are in percentage +/– standard deviation. Values in the same raw with the same superscript are not significantly different.

group. No classification was observed based on groves or sampling time, suggesting that differences between HLB, ZD, and healthy samples were greater than possible differences between groves or sampling season. Principal components (PC) 1 and 2 accounted for 56.34% of the variation and sample classification occurred mostly in the PC1. Out of the 10 compounds with the highest absolute loading values in PC1 (Figure 2B), only L-proline, unknown 20, inositol, fructose, and arabitol showed significant differences among sample groups. Analysis of variance ANOVA was run in each detected compound to find other possible

Table 3. Main compounds detected by headspace SPME*

Linear Retention Index (LRI)	Tentative identity	Relative abundance (%) ZD			HLB			Healthy		
900	4-Octene, 2,6-dimethyl-,[S-(E)]-	0,070	+/–	0,001	0,230	+/–	0,003	0,213	+/–	0,003
908	3-Octene, 2,6-dimethyl	0,053	+/–	0,001	0,147	+/–	0,002	0,305	+/–	0,003
919	α-Thujene	0,777	+/–	0,010	1,067	+/–	0,011	1,248	+/–	0,014
922	Octane, 2,6-dimethyl	0,307	+/–	0,005	0,759	+/–	0,010	0,373	+/–	0,005
934	UN1	0,513	+/–	0,004	0,835	+/–	0,007	0,860	+/–	0,005
937	UN2	0,075	+/–	0,001	0,186	+/–	0,003	0,216	+/–	0,003
946	UN3	0,138	+/–	0,003	0,424	+/–	0,004	0,518	+/–	0,007
958	2-Octene, 2,6-dimethyl	0,546	+/–	0,005	1,081	+/–	0,007	1,250	+/–	0,009
970	Sabinene	8,429	+/–	0,080	9,042	+/–	0,086	8,715	+/–	0,082
976	1,5-Heptadiene, 2,3,6-trimethyl-	0,249	+/–	0,004	0,671	+/–	0,007	0,532	+/–	0,006
980	β-Pinene	1,407	+/–	0,010	1,692	+/–	0,008	1,276	+/–	0,011
985	Trans-carane	0,000	+/–	0,000	0,247	+/–	0,003	0,190	+/–	0,003
990	2,6-Octadiene, 2,6-dimethyl-	0,585	+/–	0,005	1,098	+/–	0,006	1,147	+/–	0,007
996	1,3-Hexadiene, 3-ethyl-2,5-dimethyl-	0,445	+/–	0,004	0,550	+/–	0,005	0,732	+/–	0,004
1008	δ-3-Carene	4,659	+/–	0,044	5,360	+/–	0,046	5,159	+/–	0,050
1016	α-Terpinene	0,283	+/–	0,004	0,504	+/–	0,003	0,478	+/–	0,004
1025	Benzene, 1-methyl-2-(1-methylethyl)-	3,041	+/–	0,024	8,168	+/–	0,067	3,717	+/–	0,030
1031	*d*-Limonene	8,130	+/–	0,048	19,208	+/–	0,137	5,980	+/–	0,061
1041	1,3,7-Octatriene, 3,7-dimethyl	5,229	+/–	0,023	3,679	+/–	0,033	5,010	+/–	0,023
1059	γ-Terpinene	0,336	+/–	0,004	0,765	+/–	0,003	0,549	+/–	0,003
1088	α-Terpinolene	1,060	+/–	0,006	1,069	+/–	0,004	1,084	+/–	0,005
1096	Undecane	1,290	+/–	0,007	2,453	+/–	0,017	0,890	+/–	0,003
1152	UN4	0,508	+/–	0,004	0,771	+/–	0,006	0,465	+/–	0,002
1274	(E,E)-2,4-nonadienal	3,287	+/–	0,002	3,287	+/–	0,002	3,287	+/–	0,002
1350	α-Cubebene	0,191	+/–	0,006	0,289	+/–	0,004	0,440	+/–	0,003
1354	UN5	0,000	+/–	0,000	0,025	+/–	0,001	0,074	+/–	0,002
1365	UN6	0,000	+/–	0,000	0,030	+/–	0,001	0,221	+/–	0,002
1372	Dihydro-neoclovene (II)	0,336	+/–	0,004	0,903	+/–	0,007	0,821	+/–	0,010
1383	UN7	2,602	+/–	0,009[a,b]	2,029	+/–	0,007[a]	2,939	+/–	0,011[b]
1391	β-Elemene	26,983	+/–	0,152	14,053	+/–	0,082[a]	21,582	+/–	0,153
1396	UN8	0,185	+/–	0,003	0,497	+/–	0,005	0,655	+/–	0,006
1404	UN9	0,400	+/–	0,005	0,978	+/–	0,009	0,900	+/–	0,010
1407	UN10	0,126	+/–	0,003	0,067	+/–	0,001	0,384	+/–	0,004
1413	Ledane	1,564	+/–	0,010	2,744	+/–	0,016	3,034	+/–	0,020
1425	Trans-caryophyllene	10,471	+/–	0,028	5,408	+/–	0,029[a]	8,996	+/–	0,032
1431	Unknown 11	1,561	+/–	0,007	1,286	+/–	0,004[a]	1,678	+/–	0,007
1434	Trans-β-Farnesene	0,692	+/–	0,008[a,b]	0,382	+/–	0,004[a]	1,573	+/–	0,019[b]
1443	UN12	0,400	+/–	0,007	0,278	+/–	0,007	0,719	+/–	0,004
1448	Isocaryophyllene	0,548	+/–	0,008[a]	0,927	+/–	0,009[a]	1,442	+/–	0,008
1456	α-Humulene	3,607	+/–	0,016	1,700	+/–	0,010[a]	2,687	+/–	0,012
1467	UN13	0,072	+/–	0,002	0,123	+/–	0,004	0,390	+/–	0,004
1481	UN14	0,354	+/–	0,006	0,289	+/–	0,005	0,527	+/–	0,007
1485	β-Selinene	0,475	+/–	0,004[a]	0,416	+/–	0,006[a]	0,796	+/–	0,003
1489	α-Selinene	0,765	+/–	0,005[a]	0,692	+/–	0,008[a]	1,095	+/–	0,003
1502	δ-Cadinene	0,373	+/–	0,004	0,100	+/–	0,002	0,432	+/–	0,003

* Values are in percentage +/– standard deviation. Values in the same raw with the same superscript are not significantly different.

biomarkers among the metabolites with low loading values. While all compounds detected were present in all of the samples, significant differences were found in the concentration of several compounds. Table 2 shows the tentative identity of the most abundant compounds detected (peak to noise ratio at least of 4) as well as those compounds showing significant differences among sample groups. L-Proline and unknown 22 showed significantly higher concentrations in HLB-infected leaves when compared to the healthy and ZD-affected ones (Figure 3A). These results are in agreement with previous reports of increased proline in citrus under physiological or biological stresses. Proline accumulation in citrus (Gimeno *et al.*, 2009; Rivas *et al.*, 2008) and other plants such as sugar cane (Suriyan and Chalermpol, 2009) has been reported with stress conditions such as girdling and drought stress. Additionally, proline accumulation has also been linked to bacterial attack in other plants such as potatoes

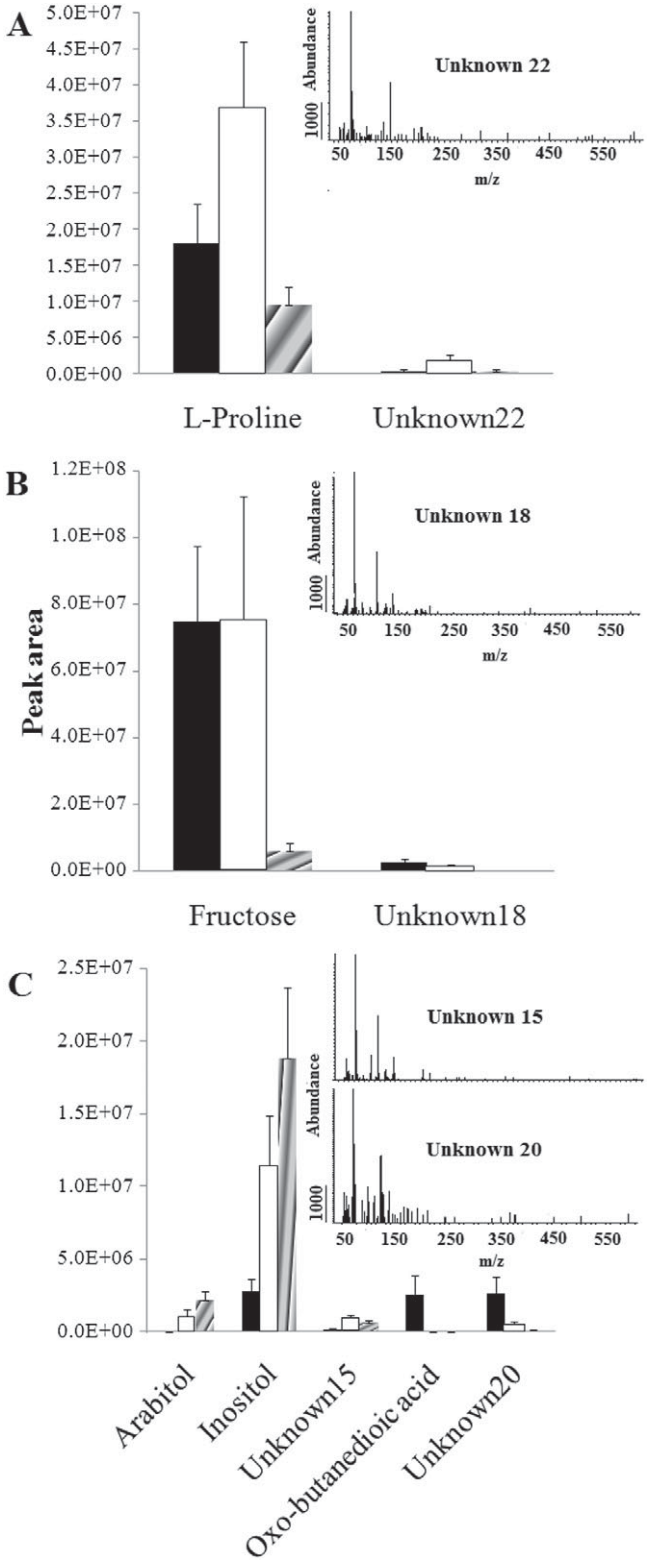

Figure 3. Compounds showing significant differences in derivatized liquid extracts of zinc deficient (■), HLB-infected (□), and healthy (◪) leaves. (A) Significantly different compounds in HLB-infected leaves only. (B) Significantly different compounds in HLB-infected and zinc deficient leaves. Figure (C) Significantly different compounds in zinc deficient leaves only. Insets show the mass spectra of each unknown compound.

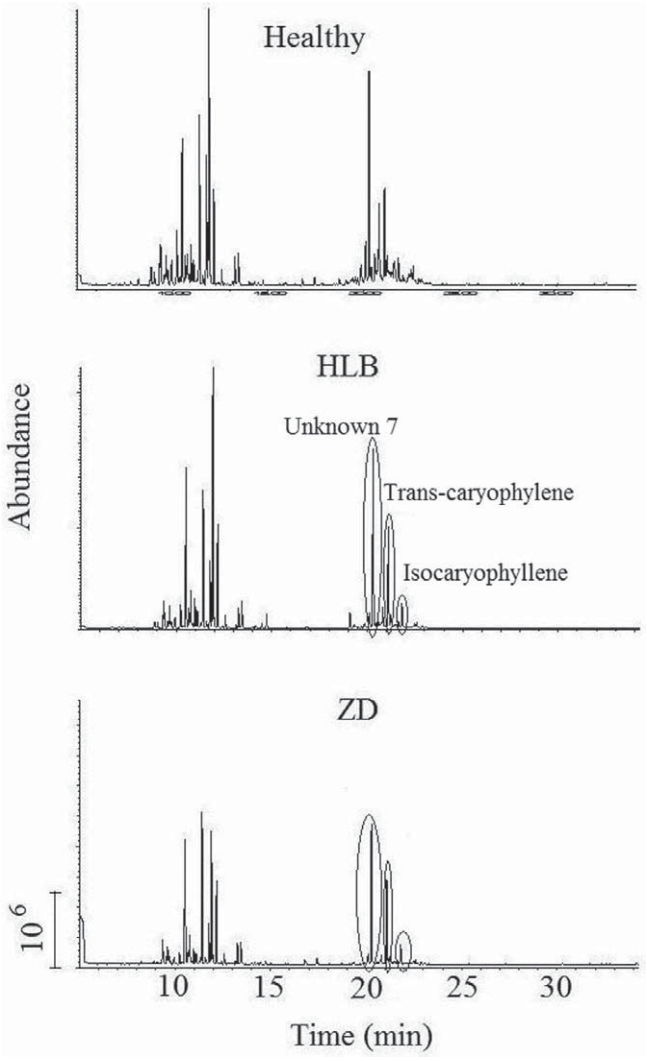

Figure 4. Typical chromatogram of SPME analyses of healthy, HLB-infected, and zinc deficient leaves. Circled compounds represent visible significant differences. Peak numbers correspond to Table 3.

(Abu-Nada *et al.*, 2007). Therefore, L-proline alone cannot be considered as an HLB-specific biomarker. Fructose and unknown 18 were in significantly higher concentration in both HLB-infected and ZD-affected samples when compared to the healthy ones (Figure 3B). Fructose may be released by sucrose synthase-mediated ADPglucose synthesis, which has been reported to be an important step in starch biosynthesis in leaves (Munoz *et al.*, 2006). This observation is in agreement with previous reports on starch accumulation in HLB infected leaves (Achor *et al.*, 2010; Etxeberria *et al.*, 2009). Starch concentration in HLB infected leaves has been reported to increase more than 10 folds (Takushi *et al.*, 2007b). Mineral imbalances, such as boron deficiency has also been shown to cause fructose accumulation in citrus (Han *et al.*, 2008). Although combined accumulation of fructose and glucose in HLB-infected plants has been reported (Dagraca, 1991), no significant differences in glucose content were detected in this study. Unknown compound 20 and oxo-butanedioic acid were in significantly higher concentrations in

zinc deficient than in healthy and HLB-infected samples whereas arabitol, neo-inositol, and unknown 15 were in significantly lower concentrations (Figure 3C).

SPME analyses

Figure 4 shows typical chromatograms of headspace analyses of leaves from healthy, HLB-infected, and ZD-affected trees. Table 3 shows the tentative identity of the volatiles detected. None of the compounds detected by SPME analyses were detected in liquid extracts, probably due to the lost of volatiles during sample drying prior to derivatization. Data show the potential of using combined headspace and liquid extracts analysis for maximizing the number of tentative biomarkers in GC-MS based metabolomic research.

As with liquid extracts, SPME data was aligned and normalized to the total area prior to statistical analysis. PCA (Figure 5A) was not able to classify the analyzed samples, suggesting similarities in the headspace metabolite profile in the sample groups. A weak discrimination of the HLB-infected samples can be seen in PC2, suggesting very small differences in the compounds with the highest PC2 loading values. Figure 5B shows the loading plot of PC1 and PC2 as well as the 10 compounds with the highest absolute PC2-loading values. Additionally, ANOVA was run for each compound to determine significant differences and possible biomarkers. Although PCA was not able to classify samples run by SPME, significant differences were found in the concentration of several headspace volatiles after running ANOVA. This shows the importance of ANOVA in metabolic differentiation studies. Table 3 shows the tentative identity of the most abundant compounds detected (peak to noise ratio at least of 4) as well as those compounds showing significant differences among sample groups. Significantly lower concentrations of several sesquiterpenes were observed in the non-healthy samples. β-Elemene, trans-caryophyllene, and α-humulene were significantly lower in HLB-infected samples only (Figure 6A), whereas isocaryophylene, α-selinene, and β-selinene were significantly lower in the HLB-infected and zinc deficient samples (Figure 6B). Decreased concentrations of sesquiterpenes has been reported in citrus with drought stress (Hansen and Seufert, 1999). The increased amounts of sesquiterpenes such as β-elemene and trans-caryophyllene detected upon infection with several pathogens such as phytoplasmas in *Hypericum perforatum* (Bruni and Sacchetti, 2005) and other plants, suggested a strong antimicrobial activity of these compounds. However, the low level of sesquiterpenes found in diseased leaves in this study, suggests an important post-infection inhibition of sesquiterpene biosynthesis upon infection, which may increase the susceptibility of 'Valencia' oranges to HLB. Recently, eight different degrees of susceptibility to this infection were characterized (Folimonova *et al.*, 2009). Further research is needed to confirm sesquiterpene inhibition in susceptible and tolerant varietes after infection with HLB.

Although the change in concentration of no single compound may be exclusively attributed to HLB, the combined use of L-proline, β-elemene, trans-caryophyllene, and α-humulene increased specificity. The combination of these biomarkers has the potential to be found with drought stress only. However, drought-affected plants don't show symptoms close to those of HLB. Hence, L-proline, β-elemene, trans-caryophyllene, and α-humulene along with visual observation of the symptoms have the potential to differentiate trees with HLB from those healthy or with zinc deficiency, the most common and HLB-similar symptomatic condition in citrus. These results complement previous work on HPLC-MS in which flavonoids and hydroxycinnamates were observed to change in HLB infected trees (Cevallos-Cevallos *et al.*, 2008; Manthey, 2008). Additionally, proposed biomarkers can be targeted by traditional chemical assays, sensors or biosensors, reducing the analysis costs and improving portability as well as rapidity. Future research is needed to determine physiological similarities between HLB and drought stress-affected plants.

Preliminary validation of HLB biomarkers

Ten samples from each treatment and each grove (total 30 samples per grove) were used to validate proposed HLB biomarkers among groves. Each of the two groves analyzed showed the same significant differences in the compounds reported in Tables 2 and 3. Peak areas were similar between groves for each proposed biomarkers, except for Unknown 22, L-proline, and Unknown 11 (Supplementary Figure 5). Same effect can be seen when comparing ratios of HLB-infected with healthy or zinc deficient samples between groves (Table 4). The differences in the concentrations and ratios of these potential biomarkers might be

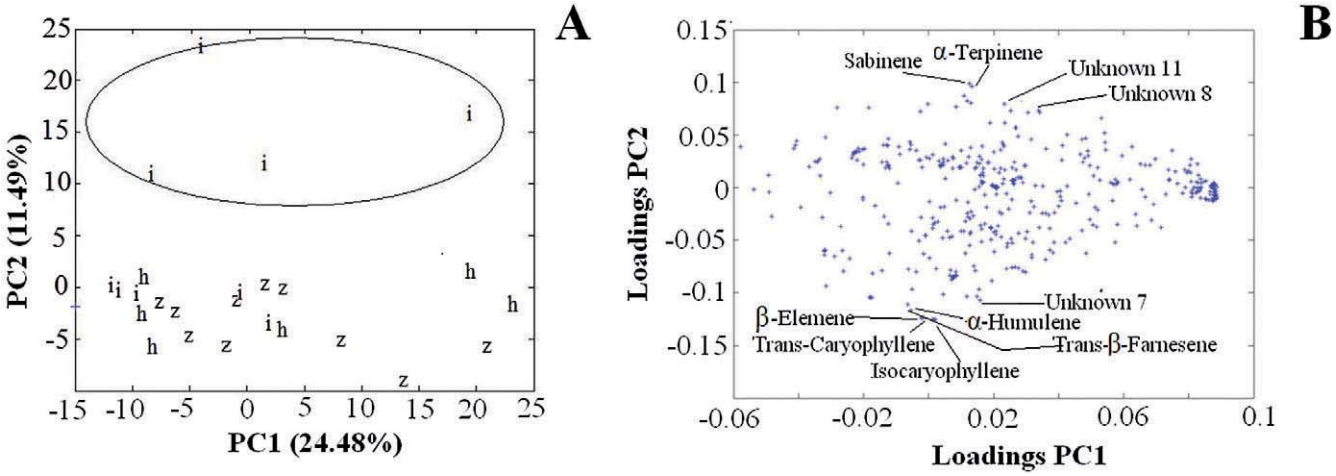

Figure 5. Principal components analysis of headspace metabolites. (A) score plot of HLB-infected (i), healthy (h), and zinc deficient (z) samples illustrated in PC1 and PC2. (B) Loading plot of PC1 and PC2. The 10 compounds with the highest absolute loadings on PC2 are marked.

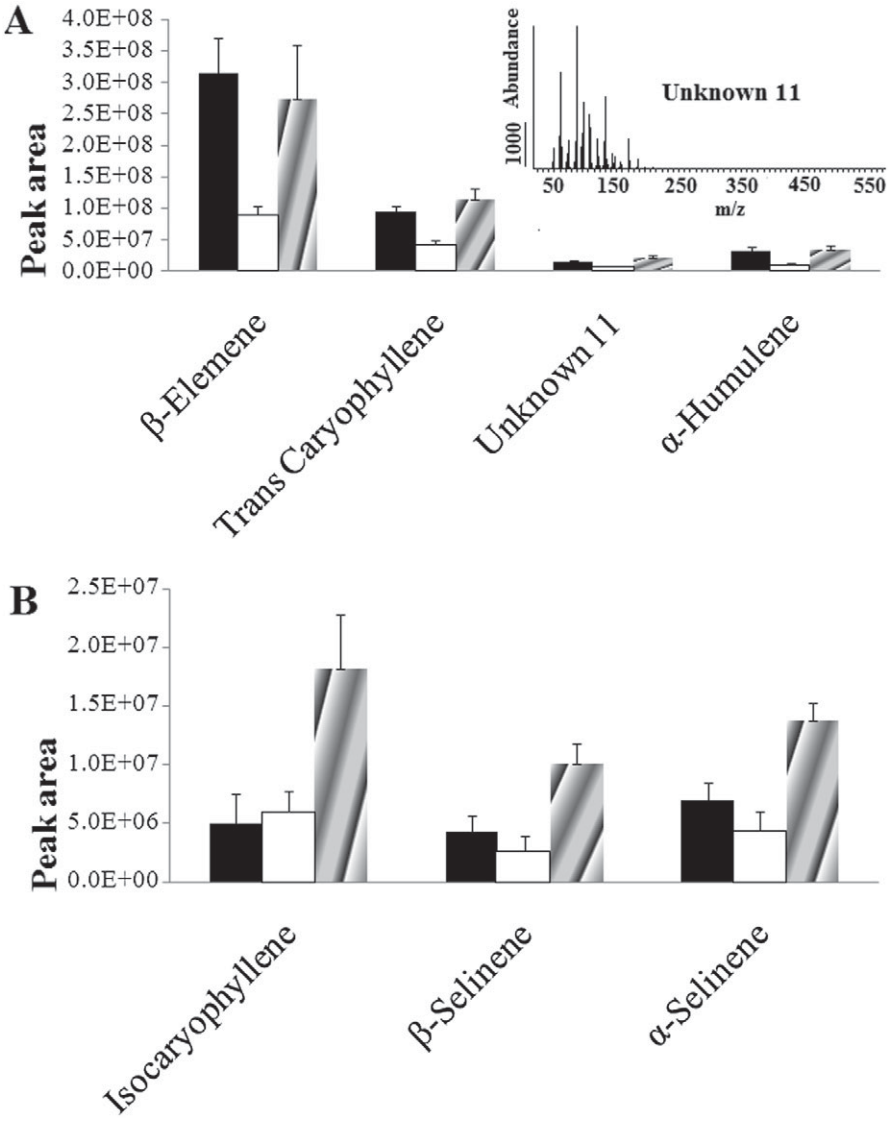

Figure 6. Significantly different headspace metabolites of zinc deficient (■), HLB-infected (□), and healthy (◪) leaves. (A) Metabolites showing significant differences in HLB-infected samples only. (B) Metabolites showing significant differences in both HLB-infected and zinc deficient samples when compared to healthy ones. The inset shows the mass spectra of the unknown compound.

Table 4. Ratios of normalized peak area of infected/healthy (i/h) and infected/zinc-deficient (i/z) of the proposed HLB biomarkers from two different groves*

	Grove 1		Grove 2	
	i/h	i/z	i/h	i/z
L-proline	6.5 +/– 1.35	3.84 +/– 1.01	4.67 +/– 0.47	5.43 +/– 1.65
Unknown 22	255.64 +/– 62.41	291.40 +/– 63.02	23.20 +/– 6.46	47.82 +/– 14.35
B-Elemene	0.52 +/– 0.19	0.74 +/– 0.21	0.56 +/– 0.43	0.68 +/– 0.38
Trans caryophylene	0.48 +/– 0.14	0.63 +/– 0.15	0.28 +/– 0.04	0.48 +/– 0.20
Unknown 11	0.28 +/– 0.03	0.65 +/– 0.35	0.58 +/– 0.20	0.64 +/– 0.11
A-Humulene	0.44 +/– 0.14	0.39 +/– 0.10	0.52 +/– 0.34	0.59 +/– 0.27

* Grove 1 = grove in Plant City, Grove 2 = grove in Lake Alfred.

due to dissimilarities in the severity of the infection. To further test this hypothesis, samples showing less severe or no symptoms from HLB-infected trees were analyzed and compared to healthy ones. Only trans-caryophyllene and α-humulene showed significant differences when comparing mildly infected with healthy leaves (Supplementary Figure 6). Therefore, the combination of all the proposed biomarkers cannot be used for HLB detection in non-symptomatic leaves. These results are in agreement with previous reports on HPLC-MS fingerprinting of HLB showing that metabolic differences are proportional to the intensity of the visual symptoms (Cevallos-Cevallos *et al.*, 2008), suggesting the need of sampling highly symptomatic leaves for metabolomic analysis. All PCR analysis performed in non symptomatic leaves were negative, showing agreement with metabolomic results. This suggests that the bacteria were probably not present in the sampled non-symptomatic leaves but changes in trans-caryophyllene and α-humulene were probably induced by the presence of the bacteria in the symptomatic leaves of the same tree. Further research is needed to better understand the response mechanism of citrus trees after HLB infection. Further validation studies involving different cultivars, groves, seasons, diseases, and stresses are needed to find HLB-specific biomarkers and determine possible metabolic differences among biotic and abiotic stresses. Additional research in greenhouse plants is needed to determine if pre-symptomatic and pre-PCR-positive changes in the metabolite profile occur in citrus.

Acknowledgements

This research was supported by grant # 00068723 from the Florida Department of Agriculture and Consumer Services and grant # 00071924 from the Florida Department of Citrus.

Literature Cited

Abu-Nada Y, Kushalappa A, Marshall W, Al-Mughrabi K, Murphy A. 2007. Temporal dynamics of pathogenesis-related metabolites and their plausible pathways of induction in potato leaves following inoculation with Phytophthora infestans. *Eur J Plant Pathol* **118**: 375–391.

Achor DS, Etxeberria E, Wang N, Folimonova SY, Chung KR, Albrigo LG. 2010. Sequence of Anatomical Symptom Observations in Citrus Affected with Huanglongbing Disease. *Plant Pathol J* **9**: 56–64.

Albrecht U, Bowman KD. 2008. Gene expression in Citrus sinensis (L.) Osbeck following infection with the bacterial pathogen Candidatus Liberibacter asiaticus causing Huanglongbing in Florida. *Plant Sci* **175**: 291–306.

Batool A, Iftikhar Y, Mughal SM, Khan MM, Jaskani MJ, Abbas M, Khan IA. 2007. Citrus greening disease—A major cause of citrus decline in the world—A Review. *Hort Sci* **34**: 159–166.

Belles JM, Garro R, Pallas V, Fayos J, Rodrigo I, Conejero V. 2006. Accumulation of gentisic acid as associated with systemic infections but not with the hypersensitive response in plant-pathogen interactions. *Planta* **223**: 500–511.

Bove J. 2006. Huanglongbing: A destructive, newly-emerging, century-old disease of citrus. *J Plant Pathol* **88**: 31.

Bruni R, Sacchetti G. 2005. Micro-organism-plant interactions as influencers of secondary metabolism in medicinal plants. *Minerva Biotecnol* **17**: 119–125.

Callaway E. 2008. Bioterror: The green menace. *Nature* **452**: 148–150.

Cevallos-Cevallos JM, Etxeberria E, Rouseff R, Reyes-De-Corcuera J. 2008. Metabolite profiling of healthy and huanglongbing-infected citrus leaves. *Proc Fla State Hort Soc* **121**: 85–89.

Cevallos-Cevallos JM, Reyes-De-Corcuera JI, Etxeberria E, Danyluk MD, Rodrick GE. 2009a. Metabolomic analysis in food science: a review. *Trends Food Sci Technol* **20**: 557–566.

Cevallos-Cevallos JM, Rouseff R, Reyes-De-Corcuera J. 2009b. Untargeted metabolite analysis of healthy and Huanglongbing-infected orange leaves by CE-DAD. *Electrophoresis* **30**: 1240–1247.

Chung K-R, Brlansky RH. 2005. Citrus diseases exotic to Florida: Huanglongbing (citrus greening). Publication #PP-210. University of Florida IFAS extension. URL [http://edis.ifas.ufl.edu/pp133]; accessed November 2009.

Dagraca JV. 1991. Citrus Greening Disease. *Annu Rev Phytopathol* **29**: 109–136.

Das AK. 2008. Huanglongbing (greening) disease of citrus: Present status and Diagnostic efforts. *Indian J Virol* **19**: 58–59.

Davis MJ, Mondal SN, Chen HQ, Rogers ME, Brlansky RH. 2008. Co-cultivation of 'Candidatus Liberibacter asiaticus' with actinobacteria from citrus with Huanglongbing. *Plant Dis* **92**: 1547–1550.

Deng CH, Zhang XM, Zhu WM, Qian J. 2004. Investigation of tomato plant defence response to tobacco mosaic virus by determination of methyl salicylate with SPME-capillary GC-MS. *Chromatographia* **59**: 263–268.

Ding F, Wang G, Yi G, Hong N, Zhong Y. 2007. Comparison of detection sensitivity of different primer pairs for citrus Huanglongbing pathogen. *Acta Phytophylacica Sin* **34**: 364–368.

Etxeberria E, Gonzalez P, Achor D, Albrigo G. 2009. Anatomical distribution of abnormally high levels of starch in HLB-affected Valencia orange trees. *Physiol Mol Plant Pathol* **74**: 76–83.

Fancy S-A, Rumpel K. 2008. GC-MS-Based metabolomics. *Methods in Pharmacology and Toxicology* 317–340.

Folimonova SY, Robertson CJ, Garnsey SM, Gowda S, Dawson WO. 2009. Examination of the Responses of Different Genotypes of Citrus to Huanglongbing (Citrus Greening) Under Different Conditions. *Phytopathology* **99**: 1346–1354.

Gimeno J, Gadea J, Forment J, Perez-Valle J, Santiago J, Martinez-Godoy MA, Yenush L, Belles JM, Brumos J, Colmenero-Flores JM *et al*. 2009. Shared and novel molecular responses of mandarin to drought. *Plant Mol Biol* **70**: 403–420.

Gopal K, Gopi V, Palanivel S, Sreenivasulu Y. 2007a. Molecular detection of greening disease in citrus by PCR: tissue source and time of detection. *Ann Plant Prot Sci* **15**: 384–390.

Gopal K, Pradeepthi ER, Gopi V, Ahammed SK, Sreenivasulu Y, Reddy MK, Baranwal VK, Purushotham K. 2007b. Occurrence, molecular diagnosis and suitable time of detection of citrus greening disease in sweet orange. *Acta Phytopathol Entomol Hung* **42**: 49–58.

Gottwald TR, Graca JVd, Bassanezi RB. 2007. Citrus Huanglongbing: the pathogen and its impact. Online. *Plant Health Progress*. doi:10.1094/PHP-2007-0906-01-RV.

Gullberg J, Jonsson P, Nordstrom A, Sjostrom M, Moritz T. 2004. Design of experiments: an efficient strategy to identify factors influencing extraction and derivatization of Arabidopsis thaliana samples in metabolomic studies with gas chromatography/mass spectrometry. *Anal Biochem* **331**: 283–295.

Hajivand S, Thohirah Lee A, Kamaruzaman S, Siti Nor AA, Nur Ashikin PA. 2009. Differential reaction of citrus species in Malaysia to Huanglongbing (HLB) disease using grafting method. *Am J Agr Biol Sci* **4**: 32–38.

Halbert SE, Manjunath KL. 2004. Asian citrus psyllids (Sternorrhyncha: psyllidae) and greening disease of citrus: a literature review and assessment of risk in Florida *Fla Entomol* **87**: 330–353.

Hall R, Beale M, Fiehn O, Hardy N, Sumner L, Bino R. 2002. Plant metabolomics: The missing link in functional genomics strategies. *Plant Cell* **14**: 1437–1440.

Han S, Chen LS, Jiang HX, Smith BR, Yang LT, Xie CY. 2008. Boron deficiency decreases growth and photosynthesis, and increases starch and hexoses in leaves of citrus seedlings. *J Plant Physiol* **165**: 1331–1341.

Hansen U, Seufert G. 1999. Terpenoid emission from Citrus sinensis (L.) OSBECK under drought stress. *Phys Chem Earth Pt B* **24**: 681–687.

Hooker ME, Lee RF, Civerolo EL, Wang SY. 1993. Reliability of Gentisic Acid, a Fluorescent Marker, for Diagnosis of Citrus Greening Disease. *Plant Disease* **77**: 174–180.

Ikeda T, Kanaya S, Yonetani T, Kobayashi A, Fukusaki E. 2007. Prediction of Japanese green tea ranking by Fourier transform near-infrared reflectance spectroscopy. *J Agr Food Chem* **55**: 9908–9912.

Kanani H, Chrysanthopoulos PK, Klapa MI. 2008. Standardizing GC-MS metabolomics. *J Chromatogr B Anal Tech Biomed Life Sci* **871**: 191–201.

Kawai T, Kikukawa K, Sasaki T, Kawazu Y, Yokoyama T, Toguchi A. 2007. Technique for detection of Huanglongbing using nested-PCR. *Res Bull Plant Prot Serv Jap* **43**: 27–32.

Li C-Y, Weiss D, Goldschmidt EE. 2003. Girdling Affects Carbohydrate-related Gene Expression in Leaves, Bark and Roots of Alternate-bearing Citrus Trees. *Ann Bot* **92**: 137–143.

Manthey J. 2008. Differences in Secondary Metabolites in Leaves from Orange (Citrus sinensis L.) Trees Affected with Greening Disease (Huanglongbing) (HLB). *Proc Fla State Hort Soc* **121**: 285–288.

McClean APD. 1970. Greening disease of Sweet Orange: its transmission in propagative parts and distribution in partially diseased trees. *Phytophylactica* **2**: 263–268.

Moalemiyan M, Vikram A, Kushalappa AC. 2007. Detection and discrimination of two fungal diseases of mango (cv. Keitt) fruits based on volatile metabolite profiles using GC/MS. *Postharvest Biol Technol* **45**: 117–125.

Munoz FJ, Zorzano MTM, Alonso-Casajus N, Baroja-Fernandez E, Etxeberria E, Pozueta-Romero J. 2006. New enzymes, new pathways and an alternative view on starch biosynthesis in both photosynthetic and heterotrophic tissues of plants. *Biocatal Biotransfor* **24**: 63–76.

Papadakis IE, Protopapadakis EE, Therios IN. 2008. Yield and fruit quality of two late-maturing Valencia orange tree varieties as affected by harvest date. *Fruits* **63**: 327–334.

Pongsuwan W, Bamba T, Harada K, Yonetani T, Kobayashi A, Fukusaki E. 2008. High-Throughput Technique for Comprehensive Analysis of Japanese Green Tea Quality Assessment Using Ultra-performance Liquid Chromatography with Time-of-Flight Mass Spectrometry (UPLC/TOF MS). *J Agr Food Chem* **56**: 10705–10708.

Rivas F, Fornes F, Agusti M. 2008. Girdling induces oxidative damage and triggers enzymatic and non-enzymatic antioxidative defences in Citrus leaves. *Environ Exp Bot* **64**: 256–263.

Sawada Y, Akiyama K, Sakata A, Kuwahara A, Otsuki H, Sakurai T, Saito K, Hirai MY. 2009. Widely Targeted Metabolomics Based on Large-Scale MS/MS Data for Elucidating Metabolite Accumulation Patterns in Plants. *Plant Cell Physiol* **50**: 37–47.

Sechler A, Schuenzel EL, Cooke P, Donnua S, Thaveechai N, Postnikova E, Stone AL, Schneider WL, Damsteegt VD, Schaad NW. 2009. Cultivation of 'Candidatus Liberibacter asiaticus', 'Ca. L. africanus', and 'Ca. L. americanus' Associated with Huanglongbing. *Phytopathology* **99**: 480–486.

Semel Y, Schauer N, Roessner U, Zamir D, Fernie AR. 2007. Metabolite analysis for the comparison of irrigated and non-irrigated field grown tomato of varying genotype. *Metabolomics* **3**: 289–295.

Suriyan C, Chalermpol K. 2009. Proline accumulation, photosynthetic abilities and growth characters of sugarcane (Saccharum officinarum L.) plantlets in response to iso-osmotic salt and water-deficit stress. *Agr Sci Chin* **8**: 51–58.

Takushi T, Toyozato T, Kawano S, Taba S, Taba K, Ooshiro A, Numazawa M, Tokeshi M. 2007a. Scratch method for simple, rapid diagnosis of citrus huanglongbing using iodine to detect high accumulation of starch in the citrus leaves. *Jpn J Phytopathol* **73**: 3–8.

Takushi T, Toyozato T, Kawano S, Taba S, Taba K, Ooshiro A, Numazawa M, Tokeshi M. 2007b. Scratch method for simple, rapid diagnosis of citrus huanglongbing using iodine to detect high accumulation of starch in the citrus leaves. *Jpn J Phytopathol* **73**: 3–8.

Tarachiwin L, Ute K, Kobayashi A, Fukusakii E. 2007. H-1 NMR based metabolic profiling in the evaluation of Japanese green tea quality. *J Agr Food Chem* **55**: 9330–9336.

Tikunov YM, Verstappen FWA, Hall RD. 2007. Metabolomic profiling of natural volatiles: Headspace trapping: GC-MS. *Methods Mol Biol* **358**: 39–53.

Urasaki N, Kawano S, Mukai H, Uemori T, Takeda O, Sano T. 2008. Rapid and sensitive detection of 'Candidatus Liberibacter asiaticus' by cycleave isothermal and chimeric primer-initiated amplification of nucleic acids. *J Gen Plant Pathol* **74**: 151–155.

Yang WL, Bernards MA. 2007. Metabolite profiling of potato (Solanum tuberosum L.) tubers during wound-induced suberization. *Metabolomics* **3**: 147–159.

Zekri M, Obreza TA. 2003. Micronutrient Deficiencies in Citrus: Iron, Zinc, and Manganese. Publication #SL 204. University of Florida IFAS Extension. URL [http://edis.ifas.ufl.edu/ss423]; accessed November 2009.

